International Journal for Housing Science and Its Applications
Publish August 10, 2025. Volume 46, Issue 4 Pages 7462-7479

https://doi.org/10.70517/ijhsa464645

Structural Design Optimization and Dynamic Characteristics Enhancement of Complex Electromechanical Equipment Based on Response Surface Methodology and Box-Behnken

Lingtao Liu[1,*]
[1] Chongqing Vocational College of Light Industry, Chongqing, 400065, China
Corresponding authors: (e-mail: t1065033160@126.com).

Abstract In order to ensure the dynamic stability of the structural design of complex electromechanical equipment, this paper proposes a structural dynamics model of complex electromechanical equipment based on Lagrange's equations and electromechanical coupling, and carries out the simulation analysis from the intrinsic frequency, accuracy, vibration behavior, and motion characteristics of complex electromechanical equipment. Then, combining the response surface method and Box-Behnken design method, the structural design of complex electromechanical equipment of high-speed rolling mill is taken as the research object, and the response surface model is established through the design variables, and the data quantitative analysis is carried out on the results of its variance optimization. It was found that in the loaded stage, the load simulation and experimental values of the spindle of the high-speed rolling mill were 45.9N·m and 48.2N·m, respectively, with an error of only 5.01%. And the optimization model R^2 and RMSE of Box-Behnken design are 0.992 and 0.004 respectively. In the structural optimization results of the high-speed rolling mill, the optimal stability can be obtained when its impact velocity is 10 rad/s, roller diameter is 6 cm, and the number of rollers is 12. Therefore, under the support of dynamics theory and response surface method, the dynamics characteristics of complex electromechanical equipment structure can be effectively explored to provide new research ideas for optimizing the structural design of complex electromechanical equipment.

Index Terms complex electromechanical equipment, response surface methodology, Box-Behnken design, Lagrange's equation, electromechanical coupling, dynamic characteristics

I. Introduction

Electromechanical equipment is one of the essential and important equipment in modern industrial production, which is widely used in various fields, including manufacturing, transportation, energy and so on. Electromechanical equipment refers to the equipment composed of mechanical part and electrical part, which plays the role of transmitting power and controlling signals in the process of industrial production [1]. As the mechanical part and electrical part are interdependent and cooperate with each other to complete the working task of electromechanical equipment, which leads to the complex internal composition of electromechanical equipment, it is prone to failure problems under prolonged use, resulting in damage to electromechanical equipment and even serious safety accidents in the operation of electromechanical equipment, which is very unfavorable to mechanized production [2], [3]. Therefore, the optimized design of electromechanical equipment structure is an effective way to solve the problem fundamentally. The development of electromechanical equipment is closely related to the progress of technology, and has now become an indispensable part of the modern industrialization process. Electromechanical equipment has a decisive role in a certain sense in the productivity, quality, cost, safety and environmental protection of industrial products [4], [5]. Therefore, the condition of various electromechanical equipment for industrial production is not only a reflection of the level of enterprise maintenance technology, but also a sign of the level of enterprise management. In addition to the optimization of the structure of electromechanical equipment itself, the kinetic characteristics of its equipment is also a hot research topic in recent years. Dynamic characteristics of electromechanical equipment refers to the mechanical system in the role of external forces, with the time change of the law of motion and mechanical properties. And the dynamic characteristics of electromechanical equipment have an important influence on the design, control and optimization of the equipment [6]. In practical applications, electromechanical equipment is often combined with computer technology to form an intelligent control system to improve production efficiency and product quality [7].

For electromechanical equipment just put into use and complex dynamic environment, did not pay too much attention to the protection and optimization design of the equipment itself, the traditional use of manual maintenance

and management optimization of its equipment protection. For example, literature [8] proposes to protect the electromechanical equipment of road tunnels by means of regular inspection, optimized management and improved maintenance to maintain its reliability and safety. The method is effective, but the efficiency is worrying, and the performance of the equipment will still decline with the flow of time. However, with the development of technology, the E&M equipment are constantly being optimized and updated. Literature [9] utilizes deep learning techniques for fault diagnosis and predictive maintenance of electromechanical equipment and incorporates optimization algorithms to optimize the process and improve the accuracy and safety of diagnosis and prediction. Further, literature [10] constructs a diagnostic optimization model for electromechanical equipment with a traditional belief rule base under the consideration of component replacement response, and conceives an expert knowledge-supported independent component analysis method to solve problems such as information redundancy in diagnosis. Similarly, literature [11] constructs a campus E&E equipment classification model by Bayesian algorithm and develops an E&E equipment safety protection system by data mining algorithm so as to optimize the safety of E&E equipment. In the electric power system, electromechanical equipment is undoubtedly an indispensable existence, and literature [12] optimized the power collection terminals in electric electromechanical equipment with the technical support of electric power communication to update and maintain the data transmission and operation management of communication and other data in the power grid. For complex electromechanical equipment, its stable and reliable operation is the basic requirement, in this regard, the literature [13] to cost as a constraint, through the multi-objective optimization algorithm and improve the bee colony algorithm to obtain the reliability model of electromechanical equipment, between the cost and the reliability of the optimal deployment scheme. The above studies, focus on the diagnosis and prediction of E&M equipment faults, and their safety and reliability. However, regarding the three aspects, direct optimization of its equipment is the main method to solve the source of the problem, and the optimal design of the structure of electromechanical equipment to a large extent increases the reliability and safety performance of the equipment itself, but there is a lack of research in this area.

In addition, in electromechanical equipment, the load change is a common kinetic properties, and its change directly affects the motion state and performance of electromechanical equipment. Literature [14] creates the concept of an adaptive sensorless system and designs an optimal energy conversion model that is commonly used to monitor the loads of electromechanical devices to understand their dynamics. In these studies, there is a lack of research on the influence of friction, lubrication, motor operating conditions, and inertia of the drive train in the dynamics, and there has not been any research on the enhancement of the dynamics of electromechanical equipment. The response surface method is able to optimize the independent variables with an effective multivariate function and obtain the optimal solution from the function locally [15]. Meanwhile, Gugulothu, B et al. combined Box-Behnken design with minimum number of experiments in multivariate function to obtain optimal conditions by response surface analysis [16]. Both of them are applicable to complex response surfaces such as morphology and structure, and can also optimize complex response variables, which provides a new idea to optimize the structure of electromechanical equipment and improve its dynamic characteristics.

In this paper, a response surface model construction method applied to the optimization of complex electromechanical equipment structure is proposed, which incorporates the Box-Behnken design scheme and solves the model by the MonteCarlo method to obtain the optimal design scheme of complex electromechanical equipment structure. In addition, the Lagrange equation is introduced as the theoretical basis, and from the electromechanical coupling of complex electromechanical equipment, the dynamics model of complex electromechanical equipment is established, and the simulation analysis is carried out for its dynamics characteristics. From the perspective of electromechanical coupling, the dynamic characteristics of complex electromechanical equipment can be effectively explored to provide support for the stable operation and optimal design of complex electromechanical equipment structures.

II. Dynamic characterization of the structural design of complex electromechanical equipment

Complex electromechanical equipment contains too many subsystems, which may fail during operation. Optimizing the structural design of complex electromechanical equipment can provide reliable help to stabilize the operation of complex electromechanical equipment. Based on this, it is necessary to fully explore the dynamics of complex electromechanical equipment structure, combined with the dynamics of complex electromechanical equipment to provide reference for the design of complex electromechanical equipment structure.

II. A.Role of complex electromechanical equipment coupling

II. A. 1) Complex electromechanical equipment systems

The modern complex electromechanical system is a complex physical system in which multiple physical processes such as machine, electricity, liquid and light are fused into a carrier, and it is also a complex equipment in which multiple unit technologies are integrated into an electromechanical carrier to form a specific function. When the equipment operates, its internal subsystems and the environment for a variety of energy, material and information transfer, conversion and evolution.

The most essential feature of the complex electromechanical system is mechatronics, which is also a modern mechanical system that fully utilizes the information processing and control functions of the electronic computer and the characteristics of the controllable drive elements to realize the intelligence and automation of the mechanical system [17]. It mainly includes three parts: control system, drive system and transmission system, and its input-output relationship and internal structure are very complex, and the various variables of the system interact with each other, which is a typical multi-input-output, nonlinear, strongly coupled, uncertainty system. Therefore, the internal structure and interaction relationship of the system cannot be fully determined by the external description alone, and there may be some variables inside the system that are not affected by external inputs or not reflected in the outputs, and there may even be some variables that are not affected by the inputs or not reflected in the outputs. The nonlinear, time-varying characteristics of the various physical processes within the system, the complex coupling between the process, the intermingling of the relationship between the control and analysis of electromechanical systems has increased the difficulty of simulating each subsystem individually, it is difficult to regulate the overall performance of the system to the optimum, and must be applied to the mechatronic integration modeling and simulation methods in order to achieve the optimization of the overall performance of the system.

There are many coupling factors in complex electromechanical systems, which have an important impact on their working state, and sometimes even cause major failures, such as a driving power of tens of thousands of kilowatts of hot rolling units in the optimal process work point due to the power supply system coupled with the mechanical system and the occurrence of strong resonance, so that the equipment is far from being able to operate at full load. A high-speed cold rolling unit, due to its work interface friction mechanism is not mastered in the nonlinear interaction law, can only run at reduced speed. A 10,000 tons of above die forging hydraulic press, in the high load, multi-flexible mechanical body between the strong power interaction, constraints on the operation accuracy, control accuracy and product accuracy.

II. A. 2) Electromechanical coupling principle of action

In the complex electromechanical equipment structure, contains a variety of types of electromechanical equipment, of which permanent magnet synchronous motor is the core component, the dynamics of the complex electromechanical equipment structure depends on the permanent magnet synchronous motor to realize. Permanent magnet synchronous motor in the permanent magnet in the air gap flux density is sinusoidal distribution, when the three-phase stator windings into the three-phase sinusoidal alternating current, after electromagnetic energy conversion in the motor internal formation of the space of uniform rotation magnetic field, and the interaction of the magnetic field of permanent magnets to form the electromagnetic torque to drive the motor rotor rotation. Further drive the transmission mechanism to drive the load movement, this dynamic process with the help of the air gap magnetic field to complete the energy conversion from electromagnetic energy to mechanical energy, there is an obvious electromechanical coupling relationship [18]. Motor in normal operation, the rotor speed is equal to the speed of the rotating magnetic field, and the speed of the rotating magnetic field depends on the frequency of the three-phase stator current, i.e., the rotor speed is strictly synchronized with the frequency of the current, and is proportional to this frequency. That is:

$$\Omega = \frac{60f}{\mu_n} \tag{1}$$

where, Ω is the motor speed, μ_n is the number of pole pairs of the motor and f is the stator current frequency.

According to the motor drag equation:

$$T - T_L = \frac{J}{9.55}\frac{d\Omega}{dt} \tag{2}$$

where J is the system moment of inertia, Ω is the motor output speed, T is the motor output torque, and T_L is the load torque.

When the motor output torque is greater than the load torque, the motor can overcome the load torque to do work. When the load torque increases, the power angle will increase with the load torque, making the input power increase,

so the stator current must also increase until the motor output torque and load torque balance. Therefore, the electrical characteristics inside the motor are often changed by the influence of external loads, and coupled with the inertia change of the connected mechanical structure and the load perturbation in the working process, the electromechanical coupling of complex electromechanical equipment systems is realized.

Complex electromechanical coupling is a basic feature of the system startup, braking and load changes and other non-stationary phase, often triggering electromechanical coupling vibration of electromechanical systems, resulting in a decline in their dynamic quality. Complex electromechanical equipment system of electromechanical coupling as shown in Figure 1, electrical parameters mainly from the drive and control of the two subsystems, mechanical parameters mainly from the mechanical transmission system and load system, both directly or indirectly through other subsystems occur electromechanical coupling, so in the study of complex electromechanical equipment system of electromechanical coupling of the vibration characteristics of the system should be comprehensively consider the mechanical and electrical system of the impact on the whole system.

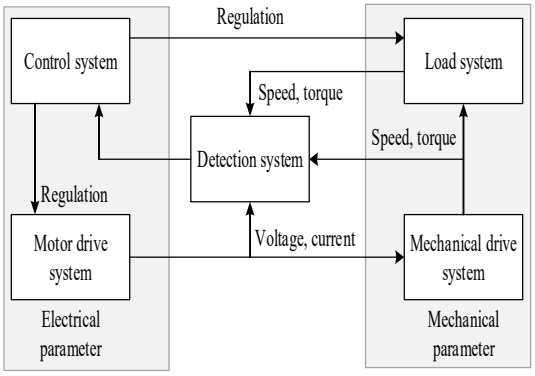

Figure 1: Coupling of electromechanical equipment

II. B.Dynamic modeling of complex electromechanical equipment

II. B. 1) Dynamic modeling theory of electromechanical equipment

The mechanical properties of complex electromechanical devices under coupling need to rely on the dynamical equations to obtain clear dynamical characteristics, which are mainly discussed in this paper from Hamilton's principle and Lagrange's equation.

If the system under study has n degree of freedom $q_j(j=1...n)$, let $L=T-V$ be the Lagrangian function, where T and V are the kinetic and potential energies of the system, respectively, and W_{nc} is the work done by the nonconservative force.Hamilton's principle can be stated as the variance of the time integral of the Lagrangian function and the nonconservative force from moment t_1 to moment t_2 equals zero. It states that in all possible motions of a conservative mechanical system subject to ideal constraints transferring from one monomorphism at moment t_1 to another monomorphism at moment t_2, the motions that actually occur cause the definite integrals of the system's Lagrangian function over that time interval to take standing values, mostly very small values. To wit:

$$\delta A=\int_{t_1}^{t_2}\delta L dt+\int_{t_1}^{t_2}\delta W_{nc}dt=0 \tag{3}$$

In many cases, for the sake of simplicity of expression, we often define the motion of a system in terms of associated degrees of freedom which are constrained by algebraic equations. Assuming that a system is represented by a vector q with n associated degree of freedom and m constraint equations $\phi_k(q,t)=0$, Hamilton's principle is expressed as

$$\delta A=\int_{t_1}^{t_2}\delta L dt+\int_{t_1}^{t_2}\delta W_{nc}dt-\int_{t_1}^{t_2}\sum_{k=1}^{m}\sum_{i=1}^{n}(\delta q_i\frac{\partial\phi_k}{\partial q_i}\lambda_k)dt=0 \tag{4}$$

The last term on the left side of the above equation can also be expressed in matrix form as $\delta q^{\tau}\Phi_q^{\tau}\lambda$, where λ is the Lagrange multiplier vector and Φ_q is the Jacobi matrix of the constraint function.

The Lagrange equations can be derived directly from Hamilton's principle. Let the kinetic energies $T=T(q,\dot{q})$ as well as $V=V(q)$, and their transformations be divided into:

$$\delta T = \sum_{i=1}^{n} \frac{\partial T}{\partial q_i} \delta q_i + \sum_{i=1}^{n} \frac{\partial T}{\partial \dot{q}_i} \delta \dot{q}_i = \delta q^T \frac{\partial T}{\partial q} + \delta \dot{q}^T \frac{\partial T}{\partial \dot{q}} \tag{5}$$

$$\delta V = \sum_{i=1}^{n} \frac{\partial V}{\partial q_i} \delta q_i = \delta q^T \frac{\partial V}{\partial q} \tag{6}$$

$$\delta W_{nc} = \delta q^T Q_{ex} \tag{7}$$

where Q_{ex} is the vector representing the external force. A direct application of the expression of Hamilton's principle follows:

$$\int_{t_1}^{t_2} \left[\delta q^T \left(\frac{\partial T}{\partial q} - \frac{\partial V}{\partial q} + Q_{ex} - \Phi_q^T \lambda \right) + \delta q^T \frac{\partial T}{\partial \dot{q}} \right] dt = 0 \tag{8}$$

The last term on the left in the above equation is obtained by applying the method of integration by parts:

$$\int_{t_1}^{t_2} \delta \dot{q}^T \frac{\partial T}{\partial \dot{q}} dt = \left[\delta q^T \frac{\partial T}{\partial \dot{q}} \right]_{t_1}^{t_2} - \int_{t_1}^{t_2} \delta q^T \frac{d}{dt} l \left(\frac{\partial T}{\partial \dot{q}} r \right) dt \tag{9}$$

Since the motion of the object is determined at the two time points of the integral, their variational components should be equal to zero, i.e., $\delta q(t_1) = \delta q(t_2) = 0$, so the first term on the right hand side of Eq. (9) is zero. Substituting Eq. (9) into Eq. (8) gives:

$$\int_{t_1}^{t_2} \left[\delta q^T \left(\frac{d}{dt} \left(\frac{\partial L}{\partial \dot{q}} \right) - \frac{\partial L}{\partial q} - Q_{ex} + \Phi_q^T \lambda \right) \right] dt = 0 \tag{10}$$

By choosing m appropriate Lagrange multiplier, we can always make the parenthesis term in the integral sign of the above equation equal to zero. I.e:

$$\frac{d}{dt} l \left(\frac{\partial L}{\partial \dot{q}} r \right) - \frac{\partial L}{\partial q} + \Phi_q^T \lambda = Q \tag{11}$$

If the quality of the system does not vary with events, the above equation can be written in the traditional form as follows:

$$M\ddot{q} + Kq + \Phi_q^T \lambda = Q_{ex} \tag{12}$$

Them and m constraint equation:

$$\Phi(q, t) = 0 \tag{13}$$

Together they form a system of $n+m$ differential algebraic equations. This system of equations is the system of equations that characterizes the dynamic response of the system.

II. B. 2) Modeling of complex electromechanical equipment dynamics

Based on the coupling relationship of complex electromechanical equipment given in the previous section and the relevant theoretical knowledge of Lagrangian dynamics, the electromechanical coupling dynamics model of the drive and transmission system of complex electromechanical equipment is established, and accordingly, the electromechanical coupling phenomenon (dynamics characteristics) existing in the structure of complex electromechanical equipment is analyzed. The following assumptions are made in the modeling process:

(1) The magnetic saturation of the permanent magnet motor and the loss of permanent magnets are negligible, and the self-inductance and mutual inductance of each phase winding are linear.

(2) The rotor of the PM motor has no eccentricity and the air gap is uniform.

(3) Neglect the influence of temperature and frequency changes on the motor parameters.

(4) Neglect the transmission clearance of the ball screw sub.

The Lagrange equation is used to establish the electromechanical coupling dynamics model of the drive and transmission subsystem of the complex electromechanical equipment system, and the Lagrange operator used can be expressed as:

$$L = T_{mech} + W_m - U_{local} \tag{14}$$

where T_{mech} represents the kinetic energy of the drive and transmission subsystem of the complex electromechanical equipment system, U_{local} represents the elastic potential energy of the drive and transmission subsystem, and W_m is the magnetic field energy of the AC permanent magnet synchronous motor.

The system Lagrange equation can be expressed as:

$$\frac{d}{dt}\left(\frac{\partial L}{\partial \dot{\wp}_j}\right) - \frac{\partial L}{\partial \wp_j} + \frac{\partial F_h}{\partial \dot{\wp}_j} = Q_j^{\varphi}, \quad j = 1,2,3,4,5 \tag{15}$$

where Q_j^{φ} is the non-conservative generalized force corresponding to the generalized coordinate $\wp_j$, and F_h is the dissipation function of the whole system.

(1) The kinetic energy of the drive and transmission subsystem of the complex electromechanical equipment system mainly includes the kinetic energy of the motor shaft rotation, the kinetic energy of the screw and the kinetic energy of the slider. So the kinetic energy of the system drive and transmission subsystem can be expressed as:

$$T_{mech} = \frac{1}{2} J_d \dot{\theta}^2 + \frac{m_s D_s^2}{16}\left(\frac{2\pi}{p}\right)\dot{Z}^2 + \frac{1}{2} m_b \dot{Z} \tag{16}$$

where J_d is the rotational inertia of the motor shaft itself, m_s is the mass of the screw, D_s is the diameter of the screw, p is the lead of the screw, and m_b is the mass of the positioning base.

(2) The magnetic field energy of the AC permanent magnet synchronous motor mainly includes the magnetic energy generated by the stator current (W_{m1}) and the magnetic energy generated by the magnetic chain produced by the rotor of the permanent magnet acting with the stator current (W_{m2}), which can be expressed as:

$$\begin{aligned} W_m &= W_{m1} + W_{m2} \\ &= \frac{1}{2}\sum_{n=1}^{3}\sum_{m=1}^{3} L_{mn} i_n i_n + i_a \psi_f \cos\theta + i_b \psi_f \cos\left(\theta - \frac{2}{3}\pi\right) + i_c \psi_f \cos\left(\theta + \frac{2}{3}\pi\right) \\ &= \frac{1}{2} L_A i_a^2 + \frac{1}{2} L_B i_b^2 + \frac{1}{2} L_C i_c^2 + H_g i_a i_b + H_g i_a i_c + H_g i_b i_c + \\ &\quad + i_a \psi_f \cos\theta + i_b \psi_f \cos\left(\theta - \frac{2}{3}\pi\right) + i_c \psi_f \cos\left(\theta + \frac{2}{3}\pi\right) \end{aligned} \tag{17}$$

In the formula, L_A, L_B, L_C respectively represents the self-inductance of the three-phase stator winding, H_g for the mutual inductance of the three-phase stator winding.

(3) Complex electromechanical equipment system drive and transmission subsystem potential energy is mainly for the torsional deformation of the ball screw sub-twisting potential energy generated by the elasticity, can be expressed as:

$$U_{local} = \frac{1}{2} K_{sc}\left(\theta - \frac{2\pi}{p} Z\right)^2 \tag{18}$$

where K_{sc} represents the torsional stiffness of the connecting sub-system of the screw.

(4) The energy dissipation part of the drive and transmission subsystem of the complex electromechanical equipment system includes the heat dissipation of the motor resistance, the rotational resistance dissipation of the motor rotor, and the frictional resistance dissipation of the motion of the positioning base on the moving guideway, which can be expressed as:

$$\begin{aligned} F_h &= F_e + F_\theta + F_Z \\ &= \frac{1}{2} R_A i_a^2 + \frac{1}{2} R_B i_b^2 + \frac{1}{2} R_C i_c^2 + \frac{1}{2} R_n \dot{\theta}^2 + + \frac{1}{2} R_f \dot{Z}^2 \end{aligned} \tag{19}$$

where R_A, R_B, R_C represents the three-phase stator resistance of the AC permanent magnet synchronous motor, respectively, R_n is the rotational resistance coefficient of the motor rotor, and R_f is the frictional resistance coefficient of the positioning base moving on the moving guide.

Substituting Eq. (16)~Eq. (19) into Eq. (15), the Lagrange operator of the drive and transmission subsystem of the complex electromechanical equipment system can be obtained as:

$$\begin{aligned} L_{local} &= \frac{1}{2}J_a\dot{\theta}^2 + \frac{m_s D_s^2}{16}\left(\frac{2\pi}{p}\right)\dot{Z}^2 + \frac{1}{2}m_b\dot{Z}^2 + \frac{1}{2}\sum_{n=1}^{3}\sum_{m=1}^{3}L_{nm}i_n i_n + i_a\psi_f\cos\theta \\ &+ i_b\psi_f\cos\left(\theta-\frac{2}{3}\pi\right) + i_c\psi_f\cos\left(\theta+\frac{2}{3}\pi\right) - \frac{1}{2}K_{sc}\left(\theta-\frac{2\pi}{p}Z\right)^2 \end{aligned} \tag{20}$$

In summary, the electromechanical coupled dynamics model of the drive and transmission subsystem in a complex electromechanical equipment system can be obtained as:

$$\begin{cases} L_A\dfrac{di_a}{dt} + H_g\dfrac{di_b}{dt} + H_g\dfrac{di_c}{dt} - \psi_f\dot{\theta}\sin\theta + R_A i_a = u_a \\ L_B\dfrac{di_b}{dt} + H_g\dfrac{di_a}{dt} + H_g\dfrac{di_c}{dt} - \psi_f\dot{\theta}\sin(\theta-\dfrac{2}{3}\pi) + R_B i_b = u_b \\ L_c\dfrac{di_c}{dt} + H_g\dfrac{di_a}{dt} + H_g\dfrac{di_b}{dt} - \psi_f\dot{\theta}\sin(\theta+\dfrac{2}{3}\pi) + R_c i_c = u_c \\ J_a\ddot{\theta} + i_a\psi_f\sin\theta + i_b\psi_f\sin(\theta-\dfrac{2}{3}\pi) + i_c\psi_f\sin(\theta+\dfrac{2}{3}\pi) + K_{se}\left(\theta-\dfrac{2\pi}{p}Z\right) + R_n\theta = 0 \\ \left[\dfrac{m_s D_s^2}{8}\left(\dfrac{2\pi}{p}\right) + m_b\right]\ddot{Z} - \left(\dfrac{2\pi}{p}\right)K_{se}\left(\theta-\dfrac{2\pi}{p}Z\right) + R_f\dot{Z} = 0 \end{cases} \tag{21}$$

From the above equation, it can be seen that the drive and transmission subsystem of complex electromechanical equipment system exists the coupling reality of AC permanent magnet synchronous motor drive current and positioning base displacement, which then affects the elastic vibration of complex electromechanical equipment structure. Therefore, the comprehensive consideration of the coupling relationship between the AC permanent magnet synchronous motor drive current and the positioning base displacement is of general and important significance to the understanding of the vibration mechanism of the complex electromechanical equipment structure, dynamic design and optimization of the system structure, and improvement of the system positioning accuracy.

III. Box-Behnken response surface methodology experimental design

After exploring the dynamics of complex electromechanical equipment systems, this chapter further introduces the Box-Behnken design in response surface methodology to explore the reliability optimization design of complex electromechanical equipment structures, which provides support for further improving the structural stability and operational reliability of complex electromechanical equipment.

III. A. Response surface methodology and fitting accuracy

III. A. 1) Response surface methodology

Due to the complexity of the structure of electromechanical equipment, its reliability function has strong nonlinear characteristics, and the relationship between the function function and random variables is often implicit. When the primary second-order moment method is used to calculate the structural reliability, it is usually required that there is an explicit relationship between the function function and the random variables. The above analysis shows that before applying the first second-order moments method to solve the structural reliability, it is necessary to transform the complex and implicit function function into a simple explicit function, and the response surface method provides a new idea for it. The basic idea of response surface method is to construct the response surface function instead of the real limit state function through a series of test points, so the main factors affecting the calculation accuracy are the selection of test points and the estimation of the response surface function [19].

(1) The linear model can be expressed as:

$$z = a + \sum_{i=1}^{n} b_i x_i \tag{22}$$

(2) The quadratic polynomial pattern without cross terms can be expressed as:

$$z = a + \sum_{i=1}^{n} b_i x_x + \sum_{i=1}^{n} c_i x_i^2 \tag{23}$$

(3) The quadratic polynomial pattern with cross terms can be expressed as:

$$z = a + \sum_{i=1}^{n} b_i x_i + \sum_{i=1}^{n} \sum_{j=1}^{n} c_{ij} x_i x_j \tag{24}$$

where n is the number of random variables and a, b_i, c_i, c_i, c_i is the coefficient to be determined.

As mentioned above, the key to calculate the system reliability based on the response surface method lies in how to construct an effective response surface function so that it is infinitely close to the real function function, and the response surface function is mostly constructed based on the test points, so the selection of the test points is also one of the main factors affecting the accuracy of the calculation results. At present, more than based on the center of the composite design selection of test points, the specific steps are as follows:

(1) Take the mean value of random variable μ_x as the initial sampling point, where $i = 1, 2, \cdots, n$, represents the number of random variables, the rest of the sampling points can be obtained by equation $\mu_{x_i} \pm f\sigma_{x_i}$, $f \geq 0$, σ_{x_i} represents the standard deviation, so the function function value of the system reliability can be determined by the above one mean point as well as $2n$ sampling points together.

(2) Calculate the uncertainty coefficients based on the real limit state function and the response surface function, and construct the response surface function $g(x)$ from them.

(3) Under the conditions of response surface function $g(x) = 0$, calculate the reliability index β and check point x^* based on the primary second-order method of moments.

(4) When the error $|\beta_k - \beta_{k+1}|$ of the first and last two times is less than the specified calculation error ε, it can be considered that the accuracy meets the requirements, and if it does not meet the conditions, then the interpolation method is used to calculate the new design point until it meets the accuracy requirements, and the interpolation formula is shown in the following equation:

$$x_i^{'} = \mu_{x_i} + g(\mu_{x_i}) \frac{(x^* - \mu_{x_i})}{g(\mu_{x_i}) - g(x^*)} \tag{25}$$

where $x_i^{'}$ denotes the new sampling point.

III. A. 2) Fitting accuracy

Before using the response surface model for optimization, it is important to evaluate the accuracy of the response surface model, and if the sample points are fitted with high accuracy, the response surface model is valid. The F-test can be used to predict the accuracy of the sample fit by testing the significance of the parameter. The basic idea of the F-test is to decompose the sum of the squares of the total deviations of the sample data into the sum of the squares of the regressions and the sum of the squares of the errors, and then find out the value of the F-value to find out the parameter of significance. The number of reductions in the sum of squares is divided by the number of independent variables added to the original model. It is usually considered that the effect of the variable on the response is significant when P<0.05, while the effect of the variable on the response is considered insignificant when P>0.05. In fact, parameter rounding can be done using stepwise regression, forward selection and backward elimination of elements, all of which are based on the F-test. In this paper, the stepwise regression method is used.

The accuracy of response surface fitting is generally determined by the experimental data. The usual criteria for testing the accuracy of response surface fitting are the residual normal distribution test, the mean of the residuals, the EISE test, the R^2 test and the relative root mean square error (RSME). For response surface models containing multiple responses and more complex models, the latter two methods are usually used to test the accuracy of the fit. The expressions for each are given below:

$$R^2 = 1 - \frac{\sum_{i=1}^{n} (\hat{y}_i - y_i)^2}{\sum_{i=1}^{n} (y_i - \overline{y}_i)^2} \tag{26}$$

$$\mathrm{RMSE}=\sqrt{\frac{\sum_{i=1}^{n}(\hat{y}_i-y_i)^2}{n-p-1}} \tag{27}$$

where $\hat{y}_i$ represents the calculated value of the response surface model, y_i represents the actual result, $\bar{y}$ represents the average value of the actual result, n represents the number of sampling points on the design space, and p represents the number of non-constant terms in the response surface mathematical model.

The R^2 coefficients and RMSE values represent the degree of difference between the response surface and the finite element analysis calculations, and their values are between 0 and 1. The closer the R^2 value is to 1, the more accurately the regressed response surface model describes the relationship between the inputs and outputs of the system within the experimental design space, and the opposite is true of the RMSE value, which is closer to 0, indicating the higher the accuracy of the model fit.

III. B. Box-Behnken response surface experimental design

III. B. 1) Defining design variables

In order to realize the optimization design of complex electromechanical equipment structure, this paper selects the electromechanical equipment of high-speed rolling mill as the research object. In this paper, through the XFlow software to get the high-speed mill stability, high-speed mill by the torque to indirectly calculate the power consumption of high-speed mill, to the bottom acceleration to express the various working conditions on the high-speed mill solid-phase movement produced by the impact of the method of applying a vertical downward acceleration, and the use of dichotomous method to indirectly measure the bottom acceleration of the high-speed rolling mill.

There are many factors affecting the structural stability of high-speed rolling mill equipment, this paper mainly from the perspective of high-speed rolling mill structural parameters and operating conditions, assuming that all other conditions remain unchanged, selected high-speed mill diameter (D), high-speed mill off the bottom of the height (H), the number of rollers (N), roller diameter (d) and high-speed mill impact speed (v) of these five parameters to establish the test of high-speed rolling mill electromechanical equipment Space.

As the quality of the high-speed mill will have an impact on the economy and power consumption of the high-speed mill system, so this paper, in addition to the above constraints on the range of values of the design variables, but also need to limit the quality of high-speed mill. The selected material is 304 stainless steel with a density of 7.92 g·cm−3. From the perspective of saving materials and reducing power consumption, the mass of the high-speed mill is generally no more than 20 kg.

III. B. 2) Response Surface Model Solving

In the response surface methodology-based modeling of complex electromechanical equipment structures in high-speed rolling mills, the iterative process is expressed as point selection, fitting, and judgment of convergence, which is repeated until the convergence criterion is met. The test sample points $(X_i^{*(k)}(t_\xi),G(X_i^{*(k)}(t_\xi)))$ as well as $(\mu_{X_i^*}(t_\xi),G(\mu_{X_i^*}(t_\xi)))$ are used as interpolated values, which are used to find the sample center for the next iteration, and the iteration criterion is defined as:

$$X_i^{*(k+1)}(t_\xi)=\mu_{X_i^*}(t_\xi)+[X_i^{*(k)}(t_\xi)-\mu_{X_i^*}(t_\xi)]\frac{G(\mu_{X_i^*}(t_\xi))}{G(\mu_{X_i^*}(t_\xi))-G(X_i^{*(k)}(t_\xi))} \tag{28}$$

There are generally three types of convergence conditions, i.e., reliability index, design point step, and design point derivative. Here the reliability index of the complex electromechanical equipment structure of the high-speed rolling mill is used, defined as β, whose geometric significance is that when a number of random variables of the structure's function function are independent of each other and obey a normal distribution, a reasonable approximation of β is the shortest distance from the origin of the test sample point $o_{\overline{x_M}}$ in the standard coordinate system to the failure boundary surface. The β in Eq:

$$\beta=\frac{\mu_G}{\sigma_G}=\frac{E[G(X_i^{*(k)}(t_\xi))]}{\sqrt{VarG(X_i^{*(k)}(t_\xi))}} \tag{29}$$

While iterating, apply the MonteCarlo method to find the reliability index of the response surface equation $\bar{G}(X)=0$ of the k st iteration $\beta^{(k)}$. Judge whether the relative error of the reliability index calculated before and after the two iterations meets the requirement, if it meets $|\frac{\beta^{(k)}-\beta^{(k-1)}}{\beta^{(k-1)}}|<\varepsilon$, ($\varepsilon$ is taken as 1% here), stop the iteration and output the response surface model.

Otherwise, make $k=k+1$ and return to continue the point selection iteration.

Combined with the reliability index of the response surface method β indicates the relationship with - probability, then the probability can be expressed as:

$$P_f=\Phi(-\beta) \tag{30}$$

where $\Phi(\cdot)$ is the cumulative probability distribution function of the standard normal distribution.

Substituting Eq. (29) into the generalized Eq. (30) yields a generalized probabilistic analytical equation based on response surface modeling for a certain type of failure or performance degradation in a t_ε-moment high-speed rolling mill complex electromechanical equipment structure as:

$$P_f(t_\varepsilon)=\sum_{i=0}^{n}\sum_{k=0}^{m}\Phi(-\frac{E[\bar{G}(X_i^{*(k)}(t_\varepsilon)\cdot\omega_{\gamma_i}\cdot\omega_{k_i})]}{\sqrt{\mathrm{var}(\bar{G}(X_i^{*(k)}(t_\varepsilon)\cdot\omega_{\gamma_i}\cdot\omega_{k_i}))}}) \tag{31}$$

IV. Simulation of dynamic characteristics of complex electromechanical equipment structural design

For the dynamic performance of complex electromechanical equipment structures, based on the coupled dynamics model of complex electromechanical equipment structures given in the previous section, this chapter verifies the intrinsic frequency, electromechanical coupled vibration characteristics and model accuracy of the design of complex electromechanical equipment structures through simulation experiments. In order to illustrate the dynamic characteristics of complex electromechanical equipment structure, and provide data reference for optimizing the design of complex electromechanical equipment mechanism.

IV. A. Intrinsic frequency and model accuracy

IV. A. 1) Device Intrinsic Frequency Simulation

For such a complex electromechanical system as a high-speed rolling mill, the previous calculation of the intrinsic frequency is carried out for a certain part of the mill, such as the roll system pendant vibration, transmission system torsion vibration, due to the structure of these systems does not exist in isolation, so there are differences compared with the real coupled system structure. Table 1 for the roll system pendant vibration, winding shaft system and the main drive subsystem intrinsic frequency and its coupling effect results, Figure 2 for the pendant vibration system speed impact response of the power spectrum, which Figure 2 (a) ~ (c) for the isolated system, coupled system and the system of the measured results, respectively.

Based on the comparison results of the power spectrum of the velocity impact response of the vertical vibration system of the high-speed rolling mill, it can be seen that the isolated system, without considering the coupling of the subsystems, its signal power fluctuation range between [-9.5,-0.1], and the overall signal power fluctuation amplitude is larger. In the complex electromechanical coupling system designed on the basis of considering the electromechanical coupling of complex electromechanical equipment structure, the signal power fluctuation range is between [-35,-30.3], and the measured signal power fluctuation range of the system is between [-35.8,-32]. The signal power fluctuation ranges of the complex electromechanical coupled system and the system measured results are more consistent. This shows that the coupling system can further enhance the response to the signal power, providing reliable data support for clarifying the power response of complex electromechanical devices.

In addition, the coupled system can be coupled together through the structure of the strip and other torsional vibration subsystems to produce frequency difference, the first and second order intrinsic frequency by the coupling of the influence of the coupling of the coupling of the two orders of the intrinsic frequency of the coupled system is much closer to the measured value than the calculated value of the isolated system. The error between the calculated and measured intrinsic frequencies of each order of the coupled system is only 0.46%, while the error between the calculated and measured intrinsic frequencies of each order of the isolated system can be up to 23.85%. Further simulation and analysis show that under the weak coupling condition, the coupling strength and frequency difference are almost monotonous, and the effect of coupling on the vibration of complex electromechanical equipment structure is completely similar to that on the intrinsic frequency, which also provides a certain arithmetic support for exploring the dynamics of complex electromechanical equipment structure.

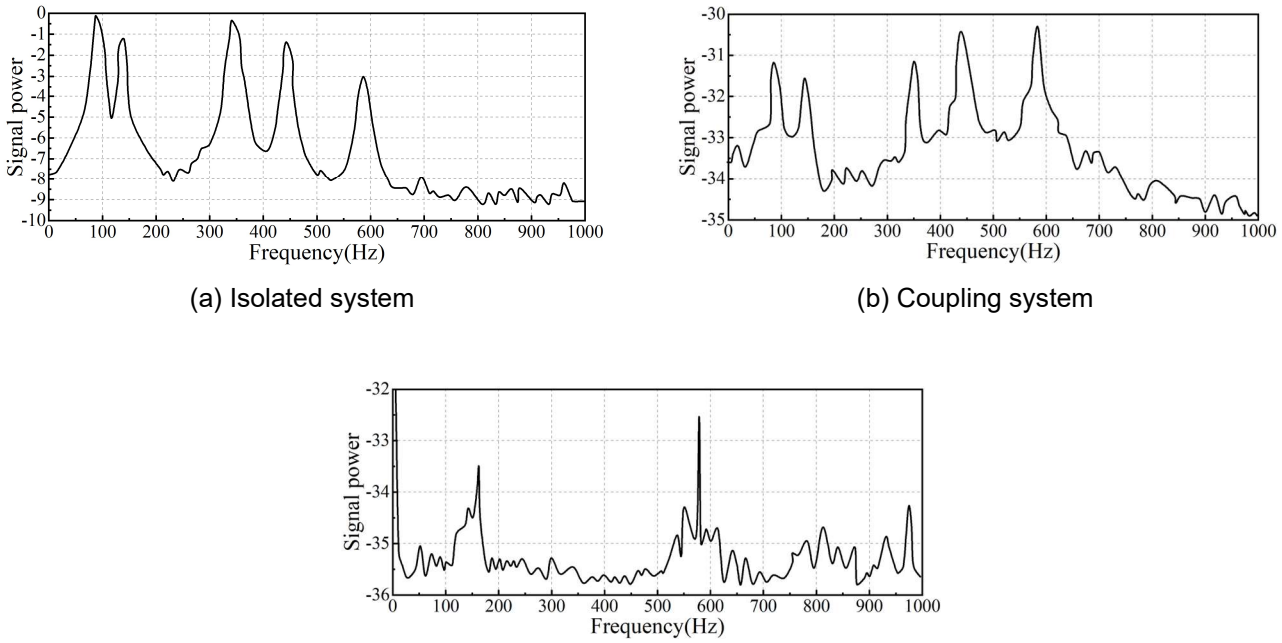

(a) Isolated system

(b) Coupling system

(c) Measured result

Figure 2: The power spectrum of the vibration system velocity shock response

Table 1: Natural frequencies and their coupling effects

Roll vibration (Hz)						
System	Ⅰ	Ⅱ	Ⅲ	Ⅳ	Ⅴ	Ⅵ
Coupling	92.36	150.29	356.24	445.63	592.18	756.45
Isolated	86.53	147.62	356.09	445.42	584.34	756.19
Measured	92.71	150.98	356.73	445.81	592.29	756.81
Coiling system (Hz)						
System	Ⅰ	Ⅱ	Ⅲ	Ⅳ	Ⅴ	Ⅵ
Coupling	16.58	39.75	65.16	185.73	325.93	459.39
Isolated	12.71	38.24	63.05	185.24	325.38	459.06
Measured	16.69	39.91	65.37	185.82	325.93	459.44
Main drive subsystem (Hz)						
System	Ⅰ	Ⅱ	Ⅲ	Ⅳ	Ⅴ	Ⅵ
Coupling	14.29	55.28	166.77	275.29	388.96	472.51
Isolated	12.01	52.39	164.69	272.38	386.52	470.37
Measured	14.38	55.34	166.78	275.42	388.98	472.72

IV. A. 2) Validation of model accuracy

Based on the dynamics model of complex electromechanical equipment structure established in the previous paper, this paper focuses on modeling the two dimensions of the permanent magnet synchronous motor and the mobile base of the complex electromechanical system of a high-speed rolling mill. For the effectiveness of the model in representing the dynamic characteristics of the complex electromechanical equipment structure, the measured impact speed and load torque of the high-speed mill are verified. Figure 3 shows the measured speed and torque results of the high-speed mill under normal condition, where Figures 3(a)~(b) show the output speed and load torque of the spindle of the high-speed mill, respectively. Among them, the complex electromechanical system of the high-speed rolling mill in the 0-30s time for the no-load stage, the load of the high-speed mill spindle is 0, and the average value of its spindle output rotational speed is 16.7 r/min. In the 30-80s time for the load stage, the average value of the load of the high-speed mill spindle is 48.2 N·m, and the average value of the output rotational speed of the high-speed mill spindle is 13.6 r /min.

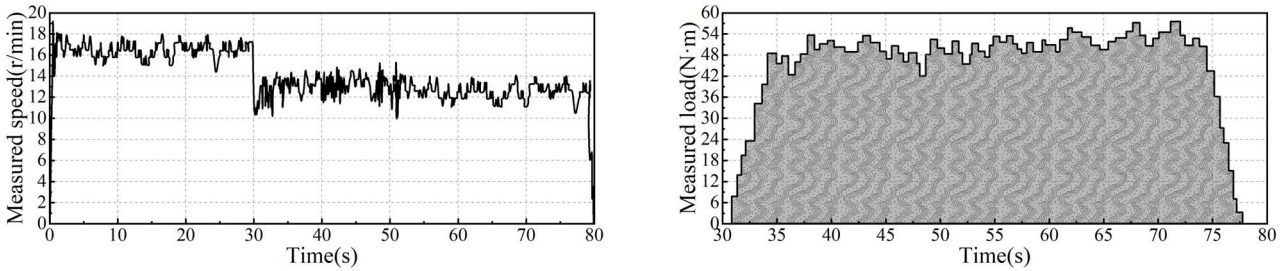

(a) The output speed of the main shaft (b) The load torque of the main shaft

Figure 3: The accuracy of the dynamic model is verified

Based on the measured results of the speed and torque of the spindle of the high-speed rolling mill under normal state, it is compared with the simulation data, and the model accuracy verification results are obtained as shown in Table 2. In the no-load stage, the output rotational speed of the high-speed mill spindle simulation value and experimental value are 17.5r/min, 16.7r/min, respectively, and the error between the two is 4.57%, the reason for the error may be:

(1) After adding the detection element in the hydraulic system, the hydraulic system damping is increased, resulting in a reduction in the system flow and a reduction in the output speed.

(2) Impurities in the lubrication of the main shaft bearings of the high-speed mill, resulting in increased friction damping and reduced output speed.

(3) Hydraulic motor after a long period of work, the internal rotor and stator may be worn, resulting in hydraulic oil leakage, the output speed is reduced.

In the load stage, high-speed mill spindle load simulation value and experimental value were 45.9N·m, 48.2N·m, two errors of 5.01%, the reason for the error may be a high-speed mill milling brought about by the load, is determined by the hardness of the rolling object and the mill feed speed, with a certain degree of uncontrollable factors The error may be due to the fact that the load brought by the high-speed rolling mill is determined by the hardness of the rolling object and the feed speed of the mill, which has certain uncontrollable factors. High-speed mill spindle output speed simulation value and experimental value of 14.1r/min, 13.6r/min, respectively, the two errors of 3.55%, the reason for the error may be:

(1) Containing the reasons generated in the no-load stage;

(2) During the experiment, the load loaded is larger than the simulation, resulting in a reduction of the rotational speed.

Comprehensive analysis shows that the experimental results of the complex electromechanical equipment structural coupling system of high-speed rolling mill are basically consistent with the model simulation results, and it can be concluded that the complex electromechanical equipment structural coupling dynamics model established in the previous paper is correct, and the simulation results are reliable.

Table 2: Model accuracy verification results

Index	Value	Load free	Load
Load (N·m)	Simulation	0.00	45.9
	Experimental	0.00	48.2
	Error	0.00%	5.01%
Speed (r/min)	Simulation	17.5	14.1
	Experimental	16.7	13.6
	Error	4.57%	3.55%

IV. B. Electromechanical coupling vibration behavior simulation

IV. B. 1) Vibration under ideal conditions

Self-synchronization of the transition process is reflected in the complex electromechanical equipment structure of the vibration system of each click and the corresponding eccentric block speed and phase change law, this transition process often appears in the vibration machinery startup process. Start due to the complex electromechanical equipment structure of the dynamic parameters and the initial conditions are not completely this, permanent magnet synchronous motor in the process of gradually accelerated to the rated speed, this change is reflected in the complex electromechanical equipment on the vibration of the direction of the angle and the amplitude of the constant change, accompanied by torque occurs. In the complex electromechanical equipment structure of the

electromechanical coupling effect, the speed of the motor and the eccentric block of the fiber gradually converge, the complex electromechanical equipment structure gradually tends to stable synchronous movement.

Ideal conditions that the complex electromechanical equipment structure of the geometric parameters of the symmetry, the parameters of the motors are identical, and the initial conditions of the system is completely symmetrical. Fig. 4 shows the simulation variation curves of the complex electromechanical equipment system under ideal conditions, where Fig. 4(a)~(f) shows the vibration displacement of the complex electromechanical equipment structure in the vertical direction, the vibration displacement in the horizontal direction, the vibration displacement in the torsion direction, the phase difference of the eccentric block on the motor shaft, the rotational speed of the motors, and the torque, respectively. As can be seen from the figure, due to the parameters of the complex electromechanical equipment structure and the initial conditions are completely symmetrical, high-speed mill in the entire start-up process of the motors have been in a synchronized state, the phase angle difference of the motors fluctuation range in the vicinity of 0, the rotational speed and torque newspaper completely has been the same, high-speed mill complex electromechanical system of the horizontal and torsion direction of vibration is 0, the vibration in the vertical direction to go through a brief transition process after the performance of a Stable periodic motion. These dynamic characteristics are completely consistent with common sense, which also indicates that the dynamic model of the complex electromechanical structure system designed in this paper can obtain ideal results under ideal conditions.

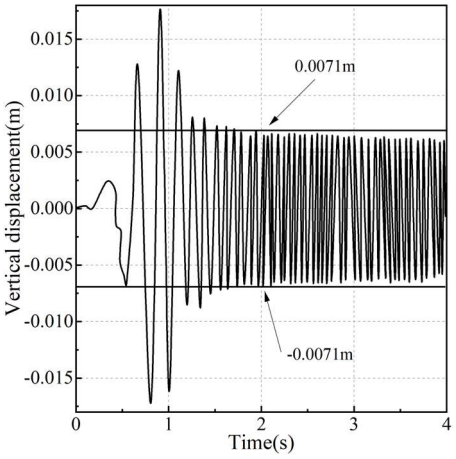

(a) Vertical direction

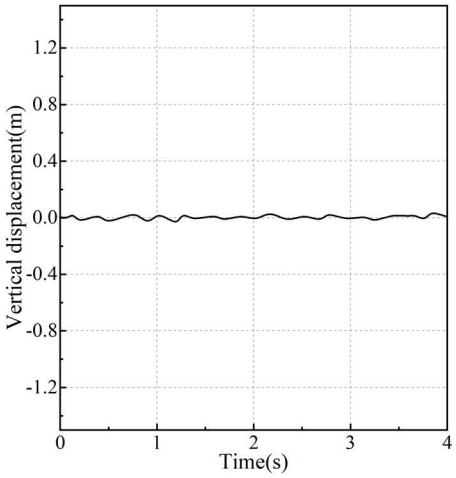

(b) Horizontal direction

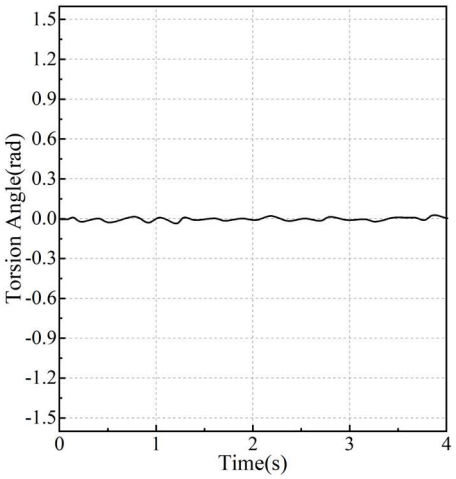

(c) Torsion Angle

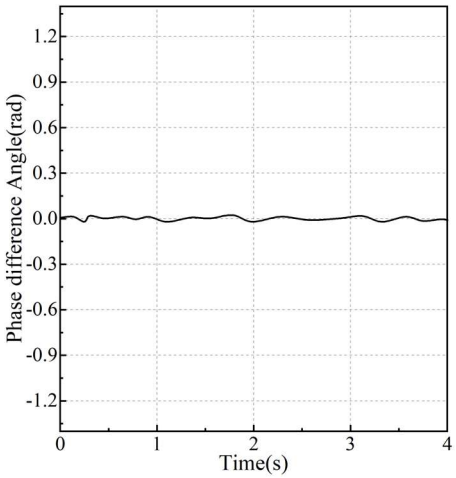

(d) Phase difference Angle

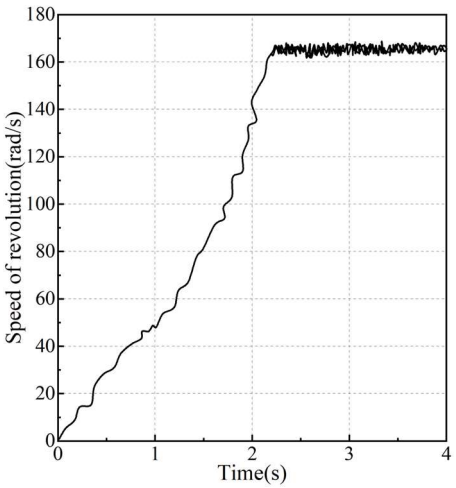

(e) Speed of revolution

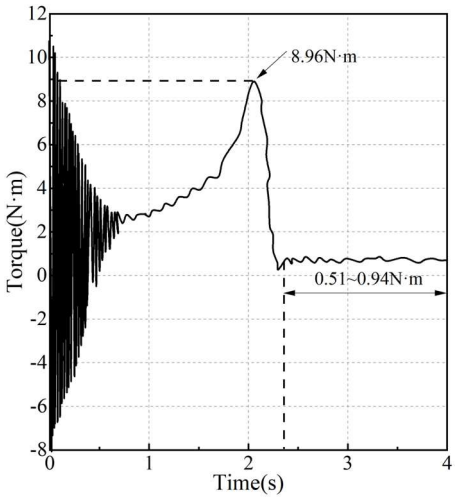

(f) Motor torque

Figure 4: The simulation curve of the ideal condition

IV. B. 2) Motion characteristics under electromechanical coupling

Based on the dynamics model of the complex electromechanical equipment structure given in the previous paper, it reflects the dynamic characteristics of the complex electromechanical equipment of the high-speed rolling mill with the dynamics of the motor and the global coupling relationship of the mechanical system. In this paper, MATLAB/Simulink is used to establish the electromechanical coupling dynamics simulation model of the complex electromechanical equipment, and the output speed of the motor and the motion speed characteristics of the moving base are solved.

(1) Output speed characteristics of the motor

Figure 5 shows the response process of the motor output speed under the action of electromechanical coupling. As can be seen from the figure, the motor speed fluctuates significantly at the beginning when the given power frequency is increased from 15 Hz to 45 Hz, and then gradually decays to approach the stable speeds of 250 r/min, 390 r/min, 500 r/min, and 620 r/min, respectively, which is consistent with the theoretical calculations, and it can be shown that the established dynamics model is correct. The results are in agreement with the results obtained from the theoretical calculations. In addition, when the time is greater than 0.225s, the change of rotational speed is small, but the value of rotational speed is not constant, but fluctuates around the target rotational speed, and the lower the target rotational speed, the greater the fluctuation amplitude. The fluctuation amplitude under different rotational speeds has some differences, but the fluctuation frequency is basically the same. And the relative speed fluctuations corresponding to the target speeds of 250r/min, 390r/min, 500r/min and 620r/min are 51.64%, 48.93%, 41.57% and 34.79%, respectively. It can be seen that the relative speed fluctuation is larger at low speeds, and the higher the target speed the relative speed fluctuation decreases.

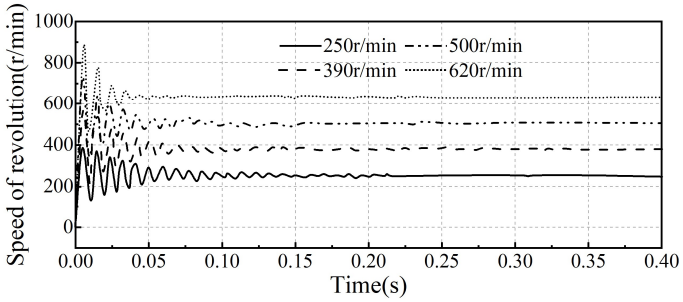

Figure 5: Motor output speed response process

(2) Movement speed characteristics of the mobile base

In the system electromechanical coupling, the output speed of the motor there are obvious fluctuations, through the role of the transmission system, is bound to have a certain impact on the movement of the mobile base. Figure 6 shows the speed characteristics of the mobile base under the role of electromechanical coupling. The motor speed of 250r/min, 390r/min, 500r/min and 620r/min corresponds to the speed of the mobile base of 0.04m/s, 0.06m/s, 0.08m/s and 0.10m/s. It can also be seen that, in the beginning stage of the movement, there are obvious fluctuations in the speed of the mobile base, and then gradually tends to be stabilized, and in the vicinity of the stabilized velocity there are certain fluctuations. And there are differences in the fluctuation amplitude of the mobile base at different speeds, but the fluctuation frequency is basically the same, and it can be seen through the relative speed fluctuation that the relative speed fluctuation is larger at low speeds, and the higher the target speed the relative speed fluctuation decreases, and this conclusion is consistent with the motor speed. Therefore, through the analysis, it can be seen that in the electromechanical coupling under the role of the motor's output speed and the speed of the moving base have certain fluctuations, is not the ideal constant speed and speed.

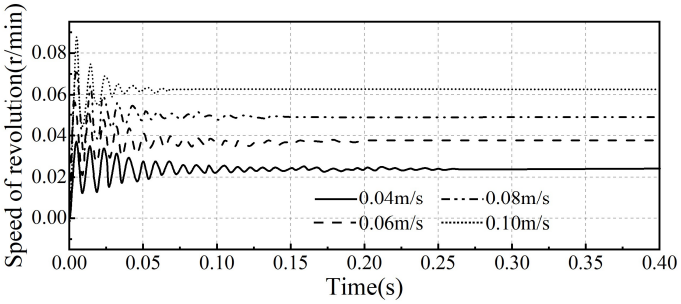

Figure 6: Motion velocity characteristics of mobile pedestal

V. Complex electromechanical equipment structure design optimization simulation verification

After clarifying the dynamic characteristics of the complex electromechanical equipment structure of the high-speed rolling mill, this paper further utilizes the Box-Behnken design of the response surface method for the optimization simulation of the structural design of the complex electromechanical equipment, which provides simulation data reference for enhancing the structural stability of the complex electromechanical equipment.

V. A. ANOVA results

In the design of complex electromechanical equipment structure of high-speed rolling mill, because the influence law between each system parameter is not a simple linear relationship, so in the establishment of the response surface model should take into account all the linear terms, square terms and the interaction between each different system parameters. In this paper, it is necessary to establish the second-order response surface model and establish the corresponding objective function, combined with the solution method and variables of the response surface model given in the previous section, the maximum equivalent stress variance of the high-speed rolling mill is analyzed, and the specific results are shown in Table 3.

As can be seen from the table, the regression model derived from the response surface model proposed in this paper for the structural design of complex electromechanical equipment of high-speed rolling mills has significant characteristics, and its sum of squares reaches 43516.09, and the P-value is 0.000<0.01. It shows that the regression model is significant at the 1% level, which also reflects a better fitting effect of the model. By analyzing the results of response surface model ANOVA, it can be concluded that in the design of complex electromechanical equipment structures of high-speed rolling mills, each different parameter has a different effect on the design effect of complex electromechanical equipment structures, and it can be found that the number of rollers in the parameter (N), the diameter of the rollers (d) and the impact velocity of high-speed rolling mills (v) have a relatively large impact on the maximum equivalent force of complex electromechanical equipment structures of high-speed rolling mills High-speed mill diameter (D), high-speed mill height from the bottom (H) on the high-speed mill complex mechanical and electrical equipment structure of the maximum equivalent force impact is relatively small.

Table 3: Max equivalent stress variance result

Item	Sum of squares	DF	Mean square	F	P
Model	43516.09	15	3125.74	12.106	0.000
D	30.58	1	30.58	0.098	0.728
H	312.63	1	312.63	1.084	0.316
N	25162.22	1	25162.22	90.214	0.001
d	15961.48	1	15961.48	56.338	0.000
v	13925.36	1	13925.36	40.014	0.000
DH	2.98	1	2.98	0.008	0.926
DN	2.75	1	2.75	0.016	0.898
Dd	5.31	1	5.31	0.002	0.991
Dv	2.14	1	2.14	0.015	0.904
HN	3.06	1	3.06	3.142	0.098
Hd	0.06	1	0.06	0.273	0.516
Hv	4.48	1	4.48	0.135	0.127
Nd	9.15	1	9.15	0.007	0.338
Nv	5.37	1	5.37	0.108	0.176
dv	6.02	1	6.02	0.232	0.329
D2	75.38	1	75.38	3.124	0.615
H2	38.97	1	38.97	0.273	0.721
N2	331.15	1	331.15	0.134	0.232
d2	226.42	1	226.42	1.147	0.295
v2	195.39	1	195.39	0.798	0.387
Residual error	3647.51	15	398.62		

V. B. Response surface model analysis and optimization

Based on the ANOVA results, the regression model is further examined, and combined with the model fitting evaluation indexes given in the previous section, the results of the response surface model for the design of complex electromechanical structures of high-speed rolling mills are obtained as shown in Table 4. Figure 7 shows the residual distribution of the model, where Figure 7(a)~(b) shows the residual normal probability distribution of the maximum equivalent stress and the residual distribution of the predicted value domain, respectively.

According to the data in the table, it can be seen that the R^2 of the model is 0.992, and its adjusted R^2 and predicted R^2 are 0.984 and 0.941, respectively, and the difference between them is less than 0.1, and its precision reaches 68.46%, which is greater than 5, indicating that the model has a certain degree of reliability.

In addition, in the residual normal distribution plot, the experimental data show irregular distribution, which meets the requirements of residual normal distribution, and the data points are evenly distributed on the diagonal, which indicates the authenticity of the experimental data. The points corresponding to the experimental values of the residuals from the predicted value domain fall on the linear regression equation, which is highly fitted to it. Moreover, the predicted and real values in the experiment are uniformly distributed on both sides of the diagonal line in a linear relationship, so the accuracy and precision of the model are good and can be used in the optimization of the design of complex electromechanical structures.

Using the response surface model to optimize the parameters affecting the complex electromechanical structure of the high-speed rolling mill, the optimization results obtained according to the regression equation are that when the impact speed of the high-speed rolling mill is 10 rad/s, the diameter of the rollers is 6 cm, and the number of rollers is 12, the maximum equivalent force of the complex electromechanical structure of the high-speed rolling mill is 97.25 N·m. The operating conditions obtained from the response surface optimization are used in the experiments, and the average value of the maximum equivalent force of the complex electromechanical structure of the high-speed rolling mill is obtained as 97.12 N·m in parallel with five experiments, which differs from the predicted value of the model only by 0.13%. Therefore, combining the response surface method with Box-Behnken design for the design of complex electromechanical structures has a certain degree of accuracy and reliability, which can lay a foundation for ensuring the stability of the design of complex electromechanical structures.

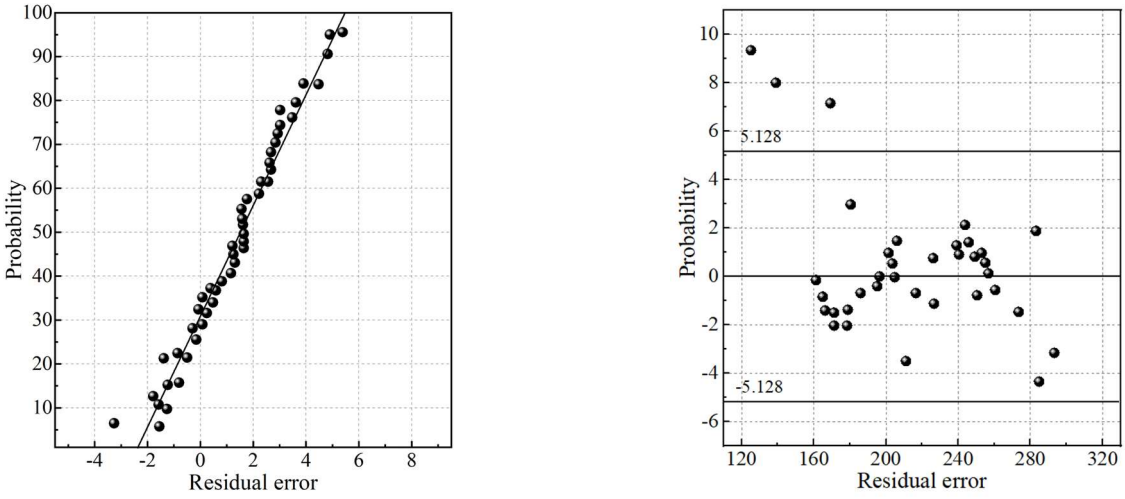

(a) Normal probability

(b) Predictive domain

Figure 7: The residual difference of the model

Table 4: Model result table

Std.Dev.	0.016	R^2	0.992
Mean	98.24	Adjust.R^2	0.984
C.V.	0.018%	Frecast.R^2	0.941
Precision	68.46%	RMSE	0.006

VI. Conclusion

The article proposes a structural design optimization model of complex electromechanical equipment based on response surface method and Box-Behnken design, and constructs a dynamics model of complex electromechanical equipment structure by combining Lagrange's equations and electromechanical coupling action, and analyzes the optimization design and dynamics characteristics of complex electromechanical equipment through simulation.

(1) In the no-load stage, the simulated and experimental values of spindle output speed of the high-speed rolling mill are 17.5r/min and 16.7r/min, respectively, and the error of both is 4.57%. In the loaded stage, the simulated and experimental values of the load of the high-speed mill spindle are 45.9N·m, 48.2N·m, respectively, and the two errors are 5.01%. Therefore, the dynamics model of complex electromechanical equipment based on Lagrange equation and electromechanical coupling effect is reliable and can accurately reflect the dynamics characteristics of complex electromechanical equipment.

(2) The R^2 of the optimization model combining response surface method and Box-Behnken design is 0.992, and its precision is 68.46%, and the RMSE of the model is only 0.004. And in the optimization results, when the impact speed of the high-speed mill is 10 rad/s, the diameter of the rollers is 6 cm, and the number of the rollers is 12, the maximum equivalent stress of the complex electromechanical structure of the high-speed mill is 97.25 N·m. The optimization results can effectively reflect the structural stability of the high-speed mill, which can better ensure the stable operation of the high-speed mill, and also provide new research ideas for the optimal design of complex electromechanical equipment structure.

References

[1] Blinov, A., & Zhukovsky, Y. (2016). Integrated system of safety and performance efficiency assessment of electromechanical equipment. Journal of Fundamental and Applied Sciences, 8(2S), 2185.

[2] Jalolov, I., Tog'ayev, A., & Eshonqulov, K. (2024). INCREASING THE ECONOMIC EFFICIENCY OF ELECTROMECHANICAL EQUIPMENT THROUGH DIAGNOSTICS OF ITS TECHNICAL CONDITION. Multidisciplinary Journal of Science and Technology, 4(12), 302-309.

[3] Wang, Y., & Wang, X. (2020). THE ON-LINE MONITORING ANALYSIS OF ELECTROMECHANICAL EQUIPMENT UNDER EMBEDDED SENSOR. International Journal of Mechatronics and Applied Mechanics, (8), 64-71.

[4] Lin, S., Luo, M., Niu, J., & Xu, H. (2022). Research on the Reliability of a Core Control Unit of Highway Electromechanical Equipment Based on Virtual Sensor Data. Sensors, 22(20), 7755.
[5] AlZohbi, G. (2018). The cost of electromechanical equipment in a small hydro power storage plant. Journal of Energy Systems, 2(4), 238-259.
[6] Mamedova, G. V. (2024). CHARACTERISTIC FEATURES OF CONTROL METHODS IN ELECTROMECHANICAL DEVICES. Reliability: Theory & Applications, 19(4 (80)), 958-966.
[7] Liu, D. (2024, January). Application of electromechanical control system based on artificial intelligence control technology. In Proceedings of the 2024 International Conference on Power Electronics and Artificial Intelligence (pp. 934-938).
[8] Chang, Q., Chen, X., Kuang, Q., & Chen, Z. (2023). Research on Maintenance and Management Optimization of Electromechanical Facilities in Highway Tunnel. Academic Journal of Science and Technology, 5(3), 169-171.
[9] Yu, T., & Xiang, X. (2024, July). Fault Diagnosis and Predictive Maintenance of Electromechanical Equipment Based on Deep Learning and Optimization Algorithm. In 2024 3rd International Conference on Artificial Intelligence and Autonomous Robot Systems (AIARS) (pp. 530-534). IEEE.
[10] Xinzhi, Y. A. O., Zhichao, F. E. N. G., Xiangyu, K. O. N. G., Zhijie, Z. H. O. U., Hui, L. I. U., & Guanyu, H. U. (2025). Multi-source information fusion based fault diagnosis for complex electromechanical equipment considering replacement parts. Chinese Journal of Aeronautics, 103420.
[11] He, A. (2024). The Security and Protection System of Electromechanical Equipment in Smart Campus using the Improved Data Mining Algorithm. Scalable Computing: Practice and Experience, 25(6), 5131-5141.
[12] Qi, C., Yang, X., Yang, X., Bi, C., & Li, W. (2024). Research on Power Line Communication Based on Deep Learning for Electromechanical Equipment Electricity Acquisition Terminals. Scalable Computing: Practice and Experience, 25(5), 3366-3375.
[13] Jianhui, D., Yanyan, L., Pengpeng, L., & Xie, H. (2021, November). Reliability Optimization Deploymentof Complex Electromechanical Equipment Based on Multi-objective Optimization Algorithm. In 2021 3rd International Conference on System Reliability and Safety Engineering (SRSE) (pp. 217-221). IEEE.
[14] Varykhalov, D. A., Pimenova, O. N., Ugarov, G. G., Moshkin, V. I., & Lappi, F. E. (2020, November). The concept of creating an adaptive sensorless system for monitoring the load of electromechanical equipment. In Journal of Physics: Conference Series (Vol. 1661, No. 1, p. 012148). IOP Publishing.
[15] Choudhary, A. K., Chelladurai, H., & Panchal, H. (2022). Optimization and prediction of engine block vibration using micro-electro-mechanical systems capacitive accelerometer, fueled with diesel-bioethanol (water-hyacinth) blends by response surface methodology and artificial neural network. Proceedings of the Institution of Mechanical Engineers, Part C: Journal of Mechanical Engineering Science, 236(9), 4631-4647.
[16] Gugulothu, B., Karumuri, S., Vijayakumar, S., Muthuvel, B., Seetharaman, S., Jeyakrishnan, S., & Saxena, K. K. (2024). Optimization of TIG welding process parameters on chrome alloy steel using Box–Behnken method. International Journal on Interactive Design and Manufacturing (IJIDeM), 18(9), 6725-6737.
[17] Minghui Wu,Wu Minghui,Wang Xuemin & Liu Xianzhong. (2020). On Condition Maintenance Model for Complex Electromechanical Equipments Based on Remaining Useful Life and Wiener Process. Journal of Physics: Conference Series(1),012014-.
[18] Susumu Minami,Tomohiro Nakayama & Takahiro Shimada. (2024). Superelastic electromechanical behaviors in ferroelectric PbTiO ceramics under coupled mechanical-electric fields: Higher-order piezoelectric constitutive equations from first-principles. Acta Materialia120248-120248.
[19] Seyedmojtaba Sajadian,Khashayar Hosseinzadeh,Shahin Akbari,Alireza Rahbari,Pouyan Talebizadehsardari & Amir Keshmiri. (2025). Discharge optimization in shell-and-tube latent heat storage systems using response surface methodology. Results in Engineering104157-104157.